PHYSICAL REVIEW B VOLUME 60, NUMBER 24 15 DECEMBER 1999-II

Ab initio study of the $CoSi_2(111)/Si(111)$ interface

R. Stadler
Institute for Physical Chemistry of the University of Vienna, Liechtensteinstrasse 22A/1/3, A-1090 Vienna, Austria and Physics and Astronomy Department, University College London, Gower Street, London WC1 6BT, United Kingdom

D. Vogtenhuber and R. Podloucky
Institute for Physical Chemistry of the University of Vienna, Liechtensteinstrasse 22A/1/3, A-1090 Vienna, Austria

(Received 17 May 1999)

An *ab initio* study based on an ultrasoft pseudopotential approach is performed for $CoSi_2(111)/Si(111)$ interfaces. Four different geometries A7, B7, A8, and B8 according to sevenfold and eightfold nearest-neighbor Co-Si interface bonding and two types of stacking are calculated. Several formulations of interface energies are considered with and without strain of the $CoSi_2$ block. The interface energy involving free surfaces without strain is chosen for deciding the stability of the interface structures. After geometry relaxation type A8 with an interface energy of 0.39 eV is the most stable interface, being more stable by 0.04, 0.06, and 0.10 eV than types B8, A7, and B7, correspondingly. By taking into account the strain energy of $CoSi_2$ a critical thickness of 150 Å of $CoSi_2$ is estimated. The relaxed interlayer spacings and atomic positions reveal strong bonding effects for interface structures A8 and B8. The good agreement of our data for structures A8 and B8 with experiment supports the view that experimentally grown interfaces are of the eightfold-coordinated type. An analysis of the electronic structure is made in terms of interface localized states. Strongly localized states are found in the Si gap of A8 and B8 interfaces. Planar-averaged densities for selected states are discussed for types A7 and A8. From the averaged metal-induced gap electron density, we derive decay lengths in Si which are significantly different, namely, about 3 Å for types A7 and B7 but much longer ranged for types A8 (about 5 Å) and B8 (about 4 Å). Schottky barriers for *p*-doped Si are derived in two different ways. The two sets of data agree reasonably showing significantly larger barrier heights for types A7 and B7 in comparison to their eightfold counterparts. The barrier heights are generally smaller than the experimentally accepted value. A correction is estimated based on quasiparticle concepts. [S0163-1829(99)02640-5]

I. INTRODUCTION

$CoSi_2$ is of interest for the design of microelectronic devices[1] because it can be grown on Si or even form buried layers in Si. Due to the small lattice mismatch and the related lattices, well-defined interfaces[2] of semiconducting Si and metallic $CoSi_2$ can be produced. The compound $CoSi_2$ has a low specific resistance at room temperature, and provides a large mean free path of about 120 Å for the electrons. Therefore, $CoSi_2$ is applied as the conducting part of metal base and permeable base transistors.[3] Extensive *ab initio* studies of the bulk and surface properties of $CoSi_2$ were presented in Ref. 4 and Refs. 5 and 6, respectively. Most of the experimental efforts studying $CoSi_2/Si$ interfaces were concentrated on the (111) orientation. As reviewed in Ref. 7, for this orientation the conditions for epitaxial growing of $CoSi_2$ on Si are favorable. Three interface types have been proposed which differ with respect to the local coordination of the Co atoms at the interface. From experimental data of transmission electron microscopy nearest-neighbor coordinations were reported to be either fivefold[8], sevenfold,[9] or eightfold.[10] Another criterion for interface geometry is established by the continuation of the stacking from one phase to the other. In so-called A-type geometry, the stacking is continued without stacking faults, whereas in the so-called B-type geometry the atomic arrangement of the $CoSi_2$ block is rotated around the [111] axis by 180° with respect to the atomic positions of the Si substrate. For the present work, calculations were performed for structures of type A7, B7, A8, and B8 where the integer defines the local coordination of Co at the interface, and A and B distinguish the two stacking variants. Interfaces with fivefold coordinated Co are not studied, since they are considered to be energetically not favorable.[11]

II. COMPUTATIONAL ASPECTS

A. *Ab initio* method

For all the calculations the Vienna *ab initio* simulation package (VASP)[12] was applied. VASP is based on an ultrasoft pseudopotentials according to Vanderbilt[13] (also see Ref. 14). Because of the concept of augmentation charges the ultrasoft pseudopotential technique is also succesfully used for the treatment of, e.g., $3d$ transition metals and their compounds,[4] and even for magnetic systems in a spin-polarized version.[15] Partial core corrections were applied according to Louie *et al.*[16] The numerical parameters and pseudopotentials were chosen in the same way as in Refs. 4 and 6. The set of **k** points was constructed according to a special **k**-point technique.[17,18] Choosing a $7\times7\times10$ grid resulted in eight **k** points in the irreducible part of the Brillouin zone, the same setting as used for studying the $CoSi_2(111)$ surface.[6] All calculations were performed within the framework of density-functional theory utilizing the generalized gradient approximation of Becke and Perdew[19] because of the excellent agreement with experimental data for bulk[4] and surface[6] properties of $CoSi_2$.

0163-1829/99/60(24)/17112(11)/$15.00 ©1999 The American Physical Society

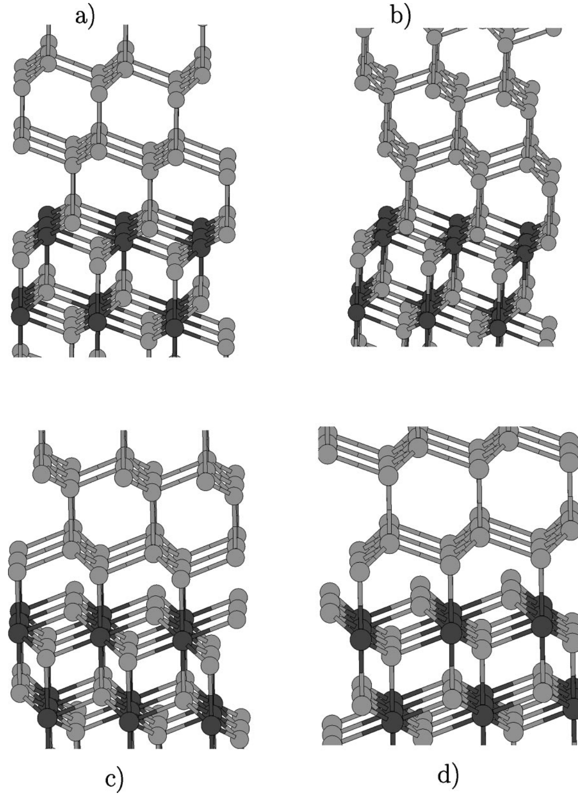

FIG. 1. Side view of the atomic arrangements for the structure types used to model the $CoSi_2(111)/Si(111)$ interface: (a) A7, (b) B7, (c) A8, (d) B8. Dark spheres: Co; light spheres: Si.

B. Geometrical aspects

Since Si crystallizes in the diamond structure and $CoSi_2$ in the CaF_2 structure, both systems have fcc sublattices. In the [111] direction, the stacking of the fcc Bravais lattice is *ABC*. The stacking sequence for the two fcc sublattices in the diamond structure is *AA-BB-CC*. In $CoSi_2$ a sequence *ABC-BCA-CAB* has to be formed to build up the correctly stacked bulk phase. The hyphens separate now trilayers of $CoSi_2$. In our calculations we used a supercell scheme where a block of $CoSi_2$ alternates with a block of Si without any vacuum layers. By construction there are then two interfaces inside the three-dimensional unit cell. For correctly deriving interface properties, it is desirable to construct unit cells in which both interfaces are equal by symmetry. Maintaining the correct stacking sequences, for types A7 and B7 the number of trilayers of $CoSi_2$ and layers of Si is then restricted to be $2m+3$ and $6n$, respectively, where m and n are integers. Five $CoSi_2$ trilayers and 12 Si layers were stacked together for the actual calculation. For type A8, $3m$ of $CoSi_2$ trilayers and $2+6n$ of Si layers are required. Now, six trilayers and 14 single layers were actually used, accordingly. Type B8 is correctly stacked by $3m$ $CoSi_2$ trilayers and $4+6n$ Si layers. We chose six $CoSi_2$ trilayers and 16 Si layers. For the actual calculation, the discussed choice of the numbers of layers amounts to 27 atoms per unit cell for A7 and B7 types, 32 atoms for A8 interfaces and 34 for B8 interfaces. All the discussed choices were made to construct the silicide blocks as thick as possible but keeping the computational efforts feasible.

Figure 1 shows side views of the four different structural types of the $CoSi_2(111)/Si(111)$ interface studied. In the following, Si positions of the blocks of $CoSi_2$ and Si directly at the interface will be denoted by $Si_C(I)$ and $Si(I)$, respectively. In general, the layers at the interface are marked by (I) and by $(I\text{-}N)$ for the Nth layer away from the interface for both blocks. For the A7 and B7 types [Figs. 1(a) and 1(b)], $Si_C(I)$ and $Si(I)$ positions have the same in-plane orientation. Whereas in the case of type A7 the stacking sequence of the Co fcc sublattice is directly continued by one of the two sublattices in the Si block, for type B7 there is a rotation of the Si block by 180° around the [111] axis. This introduces a stacking fault where $Co(I\text{-}1)$ and $Si(I\text{-}1)$ atoms have the same in-plane positions. For types A8 and B8, atoms of the $Si(I)$ layer have to be placed above $Co(I\text{-}1)$ positions. For type A8 [see Fig. 1(c)], $Si_C(I)$ sites are followed by $Si(I\text{-}2)$ sites with the same orientation. Again, if the Si block is rotated by 180° around [111], then type B8 [Fig. 1(d)] is derived from type A8.

Si is chosen to be the substrate with the two-dimensional lattice spacing corresponding to its calculated cubic bulk equilibrium spacing of 5.454 Å . The lattice mismatch of $CoSi_2$ is only 1.9 % with respect to the Si substrate, as derived from the calculated equilibrium lattice parameter of 5.350 Å for $CoSi_2$.[4] Therefore, $CoSi_2$ has to be stretched in the (111) plane and according to standard elastic behavior $CoSi_2$ has to contract in the [111] direction. A contraction of -2.3% was then derived from bulk calculations for which the planar lattice parameter for $CoSi_2$ was fixed to 5.454 Å , and the lattice spacing in [111] direction was varied until the cohesive energy was minimized. The strain energy for one bulk $CoSi_2$ trilayer amounts to 0.036 eV.

The atomic layer distance at the unrelaxed interface was chosen to be 2.36 Å for the $Si_C(I)-Si(I)$ spacing (types A7 and B7), and equally for the $Co(I\text{-}1)-Si(I)$ spacing (types A8 and B8). The fixed spacing corresponds to a perfect bulk-like continuation of the lattice of the Si block. Then, relaxation of ionic positions was allowed for ions in one $CoSi_2$ trilayer [layers Si_C, $Co(I\text{-}1)$ and $Si_C(I\text{-}2)$] and two Si layers [layers $Si(I)$ and $Si(I\text{-}1)$] next to the interface.

III. RESULTS AND DISCUSSION

A. Interface energies

All interface values in this section are defined per interface. The actual calculated results are divided by two because of two symmetric interfaces in the unit cell.

For the definition of interface energies E_{INT}, an energy reference has to be chosen. Usually either free surfaces or the corresponding bulk systems are used as references. We calculated interface energies by three different approaches: (1) from surface references without strain effects, (2) from surface references with strain added, and (3) from bulk cohesive energies as a reference.

For the derivation of $E_{INT}^{(1)}$,

$$E_{INT}^{(1)}=E_{BIND}(\mathrm{C/Si})+E_{SURF}^{0}(\mathrm{C})+E_{SURF}(\mathrm{Si}), \qquad (1)$$

two steps are considered. First, free surfaces have to be formed by cleaving the bulk materials of $CoSi_2$ and Si yielding surface energies $E_{SURF}^{0}(\mathrm{C})$ and $E_{SURF}(\mathrm{Si})$, correspondingly. The superscript 0 denotes the unstrained $CoSi_2$ mate-

TABLE I. Binding E_{BIND} and three types of interface energies E_{INT} as discussed in text for unrelaxed and relaxed geometries of $CoSi_2(111)/Si(111)$ interfaces. Unrelaxed data are denoted by (no). $E^{(1)}_{INT}$: free unstrained surfaces as reference. $nE_{STRAIN}(C)$: total bulklike strain energy for given number n of $CoSi_2$ trilayers. $E^{(2)}_{INT}$: sum of $E^{(1)}_{INT}$ and total strain energy. $E^{(3)}_{INT}$: derived from unstrained bulk cohesive energies. The strain energy per $CoSi_2$ trilayer is 0.036 eV. All energy values are in eV.

	A7	B7	A8	B8
E_{BIND}(no)	-1.64	-1.60	-1.45	-1.52
E_{BIND}	-1.75	-1.71	-1.81	-1.77
$E^{(1)}_{INT}$(no)	0.56	0.60	0.75	0.68
$E^{(1)}_{INT}$	0.45	0.49	0.39	0.43
n	5	5	6	6
nE_{STRAIN}(C)	0.18	0.18	0.22	0.22
$E^{(2)}_{INT}$	0.63	0.67	0.61	0.65
$E^{(3)}_{INT}$	0.71	0.76	0.65	0.63
E_{INT} (Ref. 11)	0.86	-	0.68	0.53

rial. Si is always in its unstrained state according to Sec. II B. Values of 0.85[6] and 1.35 eV were derived for $E^{0}_{SURF}(C)$ and $E_{SURF}(Si)$, respectively, for the unrelaxed surfaces. The actual values of E_{SURF} were derived from the differences of cohesive energies of the corresponding slabs minus the bulk values.[6] In the second step, blocks of $CoSi_2$ and Si are matched together forming a multilayer structure. The surfaces of the blocks bind together with energy $E_{BIND}(C/Si)$ which is defined by the difference of the cohesive energies F of the interface system and of the two surfacelike slabs within the same unit cell:

$$E_{BIND}(C/Si)=F_{BIND}(C/Si)-F_{SURF}(C)-F_{SURF}(Si). \tag{2}$$

These slabs were created by either removing the Si block or the $CoSi_2$ block from the original multilayer interface system. Note that $F_{SURF}(C)$ is now calculated for the strained geometry of the $CoSi_2$ block. Because in Eq. (2) the unit cell is the same for all quantities, the numerical accuracy is comparable, yielding reliable energy differences. If—as was done for calculating E_{SURF}—the unrelaxed surface geometries for $F_{SURF}(C)$ and $F_{SURF}(Si)$ are also chosen, then the interface energy is independent of the state of relaxation of the free surfaces. For that statement we have implicitly assumed that E_{SURF} and F_{SURF} are of comparable numerical accuracy.

The definition of interface energy by Eq. (1) has the advantage that it is independent of the strain energy of the $CoSi_2$ block Therefore, it serves as a well-defined quantity independent of the number of actual layers involved in the calculation (assuming that the blocks are sufficiently thick so that the interfaces do not interact significantly). If the strain of n $CoSi_2$ trilayers is taken into account, then the energy

$$E^{(2)}_{INT}=E^{(1)}_{INT}+nE_{STRAIN}(C) \tag{3}$$

is derived (see Table I).

A third definition which is quite often applied is made via bulk cohesive energies by the differences of cohesive energies of the interface system, F_{INT} and the corresponding bulk values F_{BULK}:

$$E^{(3)}_{INT}=F_{INT}(C/Si)-F^{0}_{BULK}(C)-F_{BULK}(Si). \tag{4}$$

Table I presents interface and binding energies for the unrelaxed and relaxed $CoSi_2(111)/Si(111)$ ionic positions at the interface. The binding and interface energies after relaxing the atomic positions at the interface are rather close, varying within 0.1 eV. Taking the values of $E^{(1)}_{INT}$ as the best-suited set of data for comparing interface energies, we find that structure type A8 is the energetically most favorable interface, but that the value for type B8 is only larger by 0.04 eV. The sevenfold structure types are less favorable; type A7, however is only less stable than type B8 by 0.02 eV.

If numerical accuracies are comparable, the energies $E^{(2)}_{INT}$ and $E^{(3)}_{INT}$ should be the same, but some significant differences are found for A7 and B7. $E^{(3)}_{INT}$ for A7 and B7 is about 10% larger than $E^{(2)}_{INT}$. However, the values for the A8 and B8 interfaces are very close. Considering the $E^{(2)}_{INT}$ data type A8 would be favorable in contrast to $E^{(3)}_{INT}$, which shows a ''preference'' for type B8 by 0.02 eV. The results for $E^{(3)}_{INT}$ should be less precise than for $E^{(2)}_{INT}$ because the numerical treatment for the different subsystems is different (e.g., for the construction of Fourier grids). However, it should also be noted that the strain energy was calculated for a perfect bulk material. For layers closer to the interface strain energy might be different, although one would not expect significant differences.

Table I also presents values of the pioneering *ab initio* calculations by Hamann,[11] which are different compared to our data. In Ref. 11 the studied interface system was much smaller, and the interfaces were built up only by two $CoSi_2$ trilayers and two layers of Si. Also, there are only interface layers in this structural model. Furthermore, no relaxation or strain effects were considered in Ref. 11 either. Certainly, with our more elaborate model for the interface system we will achieve more realistic results in comparison to Ref. 11.

van den Hoek *et al.*[20] performed lowest combination of atomic orbitals calculations modeling $CoSi_2(111)/Si(111)$ interfaces by clusters containing only one Co atom and one nearest-neighbor shell of Si atoms with saturated dangling bonds. Based on results for this model, it was argued that interface types with eightfold-coordinated Co positions should be more stable because a dangling bond of Co 3d character would then be saturated. In contrast, it was claimed that this is not the case for $NiSi_2(111)/Si(111)$ interfaces because the d band is filled. However, as was already discussed in Ref. 6, the bonding in $CoSi_2$ and related interfaces is more complex and cannot be reduced to covalent Co-Si bonds only, because Si-Si bonds also play an important role. As will be discussed in Sec. III B the bonding at the interface is even more complex.

Recent experimental findings[21] indicate that for epitaxially grown $CoSi_2$ films on Si(111) substrates eightfold-coordinated Co positions are more likely to be found than sevenfold-coordinated ones. However, since the interface energies of types A8, B8, and A7 are only different in the range

TABLE II. Bulk and relaxed interlayer spacings in Å for the $CoSi_2(111)/Si(111)$ interfaces. Experimental values taken from Ref. 21. First line: relaxed interlayer spacing closest to the center of the Si block; last line: relaxed interlayer spacing closest to the center of the $CoSi_2$ block. The $Si(I)-Si_C(I)$ spacing directly at the interface is accentuated by horizontal lines.

Spacing	Calculation					Expt.
	bulk	A7	B7	A8	B8	B8
$Si(I\text{-}2)-Si(I\text{-}1)$	2.36	2.40	2.39	2.30	2.29	-
$Si(I\text{-}1)-Si(I)$	0.79	0.81	0.81	0.84	0.82	0.57
$Si(I)-Si_C(I)$	-	2.41	2.40	1.87	1.91	1.82
$Si_C(I)-Co(I\text{-}1)$	0.77	0.72	0.75	0.44	0.43	0.53
$Co(I\text{-}1)-Si_C(I\text{-}2)$	0.77	0.60	0.57	0.87	0.87	0.92
$Si_C(I\text{-}2)-Si_C(I\text{-}3)$	1.54	1.65	1.66	1.49	1.49	1.52

of a few hundredths of an eV according to Table I, kinetics might play an important role for the actual growth process. From Table I it can be realized that by viewing binding and interface energies, the sequence of the structure types is changed by relaxing the layers next to the interface. As described in Sec. II B, the values for the unrelaxed cases are somewhat artificial due to the choice of spacing between interface layers.

A critical number n_{CRIT} of strained $CoSi_2$ layers may be defined by

$$E_{CRIT}=E_{BIND}(\mathrm{C/Si})+n_{CRIT}E_{STRAIN}(\mathrm{C})\geqslant 0, \qquad (5)$$

when the critical energy E_{CRIT} becomes positive. Then the energy loss for straining all $CoSi_2$ trilayers in the cell compensates the energy gain due to formation of chemical bonds at the interface. For the studied systems this balance will be reached for $n_{CRIT}\sim 48$, which would be equivalent to a thickness of ~ 150 Å of strained $CoSi_2$.

B. Interlayer spacing and local bonding

In Table II the calculated interlayer distances after relaxing the ionic positions for all four interface types are given and compared to experimental data (Ref. 21) for B8. As revealed by Table II, there are rather small differences between data corresponding to the same sevenfold- or eightfold-coordinated interface types. The spacings between $Si_C(I)$ and $Si(I)$ layers for types A7 and B7 are very similar to the corresponding distances in bulk Si. However, for types A8 and B8 the interlayer spacing at the interface is strongly reduced by about 25% of the bulk value indicating strong bonding.

For all interfaces, the changes of spacings in the Si block compared to the bulk values are rather small. With the exception of the slightly reduced $Si(I\text{-}2)-Si(I\text{-}1)$ distances for types A8 and B8, all remaining layer distances are weakly increased. It should be noted that the $Si(I\text{-}2)$ layer is kept fixed during ionic relaxation representing the bulk termination of the Si block.

Inspecting the calculated data for the $CoSi_2$ block, for types A8 and B8 a very pronounced contraction of the $Si_C(I)-Co(I\text{-}1)$ distance is found. Again, such a strong bonding feature is absent for types A7 and B7. Furthermore, the variations of the $Co(I\text{-}1)-Si_C(I\text{-}2)$ and $Si_C(I\text{-}2)-Si_C(I\text{-}3)$ distances are of distinctly oscillating character: for A7 and B7 the first distance is contracted and the latter one stretched, whereas for types A8 and B8 the situation is reversed. Bulk termination is defined by fixing the positions of layer $Si_C(I\text{-}3)$.

The comparison of the calculated data to the low-energy-electron-diffraction (LEED) data of Ref. 21 for B8 shows very good agreement except for the $Si(I\text{-}1)-Si(I)$ distance. The LEED measurements were performed for a surface system consisting of an average of 2.2 $CoSi_2$ trilayers on Si(111). The evaluation was carried out with quantitative structural LEED tensor analysis.[22] Since this method becomes less reliable with increasing distance from the surface, it is plausible that the experimentally derived layer distance deeper down in the substrate cannot be determined accurately. On the other hand, our calculation refers to a multilayer system without any surface. However, since we find only small changes of interlayer distances for the Si block, we argue that our modeling of the Si substrate by a finite number of layers is reliable. It is interesting to note that the data of the $CoSi_2$ blocks are in such a good agreement because there the changes with respect to the bulk are large and the experimental data refer to atomic layers only one $CoSi_2$ trilayer below the surface.

The bonding at the interface is reflected by the local atomic coordinations. Table III summarizes the number of neighboring atoms up to a distance of 3.0 Å for atoms next to the interface, together with the corresponding bond lengths for all four interfaces.

Within the $CoSi_2$ block the eight Co-Si bonds per Co atom are separated into two different sets of bond lengths because, due to the small lattice mismatch, $CoSi_2$ has to be stretched parallel to the interface plane and contracts perpendicular to it. Compared to the equilibrium bulk value of 2.32 Å,[6] in strained $CoSi_2$ there are six Co-Si bonds of length 2.36 Å and two of length 2.31 Å. The six Si_1-Si_2 nearest-neighbor bonds connecting the two different Si sublattices in $CoSi_2$ made an important contribution to the cleavage energy.[6] Their equilibrium length of 2.68 Å corresponds to a value of 2.71 Å for the strained case. The Si block is assumed to be in its bulk equilibrium with four Si-Si nearest neighbor bonds per unit cell each of the length of 2.36 Å.

For types A7 and B7 the local environment is nearly identical, according to Table III. These two interface structures differ only for shells of neighbors much more distant than 3.0 Å. Whereas for type A7 each $Co(I\text{-}1)$ atom has three $Si(I\text{-}1)$ neighbors in a distance of 4.51 Å, for type B7 there is only one such neighbor in a distance of 3.96 Å. As in bulk Si, for both structure types the positions of $Si(I)$ and $Si(I\text{-}1)$ of the Si block are surrounded by four Si neighbors. However, these positions are not equivalent anymore but the bond lengths are very similar. The $Si_C(I)$ atom now loses three of its original six Si_C neighbors. Therefore, the distance of this atom with respect to the remaining three Si neighbors is reduced by 0.12 Å, which seems to be one of the dominating bonding effects. All three neighbors are equivalent to position $Si_C(I\text{-}2)$ which has the same local environment as in bulk $CoSi_2$. However, since its distance from $Si_C(I)$ is re-

TABLE III. Number of symmetry-equivalent neighbors N and bond lengths d in Å for atomic positions next to the interface. Bond lengths are given for relaxed geometries. The change due to relaxation Δ is given in parentheses: +, elongation; –, contraction.

	N	$d(\Delta)$			
		A7	B7	A8	B8
Si(I-1)	3(Si)	2.37(+0.01)	2.37(+0.01)	2.38(+0.02)	2.37(+0.01)
	1(Si)	2.40(+0.04)	2.39(+0.03)	2.30(−0.06)	2.29(−0.07)
	1(Si)	–	–	2.71(+0.33)	–
Si(I)	3(Si)	2.37(+0.01)	2.37(+0.01)	2.38(+0.02)	2.37(+0.01)
	1(Si)	2.41(+0.05)	2.40(+0.04)	–	–
	3(Si)	–	–	2.91(+0.17)	2.93(+0.19)
	1(Co)	–	–	2.31(−0.05)	2.34(−0.02)
$Si_C(I)$	3(Co)	2.34(−0.02)	2.35(−0.01)	2.27(−0.09)	2.27(−0.09)
	3(Si)	2.59(−0.12)	2.59(−0.12)	2.59(−0.12)	2.58(−0.13)
	3(Si)	–	–	2.91(+0.17)	2.93(+0.19)
	1(Si)	2.41(+0.05)	2.40(+0.04)	2.71(+0.33)	–
Co(I-1)	3(Si)	2.31(−0.05)	2.30(−0.06)	2.27(−0.09)	2.27(−0.09)
	3(Si)	2.34(−0.02)	2.35(−0.01)	2.40(+0.04)	2.39(+0.03)
	1(Si)	2.26(−0.05)	2.24(−0.07)	2.37(+0.06)	2.36(+0.05)
	1(Si)	–	–	2.31(−0.05)	2.34(−0.02)
$Si_C(I-2)$	3(Co)	2.31(−0.05)	2.30(−0.06)	2.40(+0.04)	2.39(+0.03)
	1(Co)	2.42(+0.11)	2.44(+0.13)	2.26(−0.05)	2.26(−0.05)
	3(Si)	2.59(−0.12)	2.59(−0.12)	2.59(−0.12)	2.58(−0.13)
	3(Si)	2.77(+0.06)	2.78(+0.07)	2.68(−0.03)	2.68(−0.03)

duced drastically, the bond length to Co and Si positions inside the $CoSi_2$ block is enlarged.

For type A8, the atoms in layers Si(I) and Si(I-1) are now overcoordinated as compared to the tetrahedral environment in bulk Si. The atom Co(I-1) has its full bulk coordination, and $Si_C(I)$ loses one Co neighbor but has now seven Si neighbors. The strongest relaxation effect can be seen in the increased distance between Si(I-1) atoms of the Si block and the $Si_C(I)$ positions. However, the resulting distance is still only 2.71 Å, which corresponds to the Si-Si bond length in bulk $CoSi_2$. Based on local bonding arguments, this single bond is the only criterion allowing a distinction between structures A8 and B8. The interaction between $Si_C(I)$ and Si(I) is obviously repulsive, since corresponding distances increase to 2.91 and 2.93 Å for types A8 and B8, respectively.

It can be concluded that for types A7 and B7 the bonding in the Si block remains essentially unchanged compared to the bulk. The interface positions of the $CoSi_2$ block are undercoordinated, whereby Co(I-1) loses one Si neighbor and $Si_C(I)$ loses one Co neighbor and three Si neighbors. For types A8 and B8, positions on both sides of the interface are overcoordinated and a competition between stabilizing additonal bonding and destabilizing repulsive effects can be assumed. These effects more or less outweigh each other, since the interface and bonding energies of all four systems are very close to each other.

C. Energy Bands

Figures 2(a) and 2(b) show the projected bands of bulk $CoSi_2$ and bulk Si in which for all cases [and also for Figs. 2(c) and 2(d)] the Fermi energy E_F is the zero of the energy scale. For perfect bulk Si the Fermi energy is defined by the top of the valence band. As a reference system we brought bulk $CoSi_2$ and bulk Si in thermodynamical equilibrium to each other without allowing any interaction, which was done by setting the chemical potentials, i.e., the Fermi energies of both systems, equal. By this construction the projected band structures [as applied in Figs 2(c) and 2(d)] are overlapped. Features of the band structure such as interface states due to the chemical interaction at the interfaces can then be directly realized from Figs. 2(c) and 2(d), in which the sum of projected bands of the pure bulk systems are superposed by the energy bands of the interface calculations. The bulk band structure of Si (Fig. 2b) reveals wide partial gaps for the occupied states. We find localized features, which we exploit in Sec. III E for the derivation of Schottky barriers later on: at $\bar{K}$ the two lowest areas of band projections shrink to points at -8.6 and -6.7 eV. The fundamental indirect gap near to $\bar{M}$ on the direction $\bar{\Gamma}$-$\bar{M}$ is about 0.5 eV, about half of the experimental value. As is well known, the gaps calculated from ground-state density functional theory are often too small. For a correct calculation of the gap size, excitations must be described properly.

The bulk band structure of $CoSi_2$ shows much smaller gaps with a wide partial gap above the Fermi energy for direction $\bar{M}$-$\bar{K}$. At E_F around $\bar{\Gamma}$ no gap occurs, demonstrating the metallic character of $CoSi_2$. Again as in Si, localized features of bands merging into a point are found at $\bar{K}$ now at about -1 eV.

The calculated bulk band structure of Ref. 23 was quite often used for searching for a possible ballistic electron

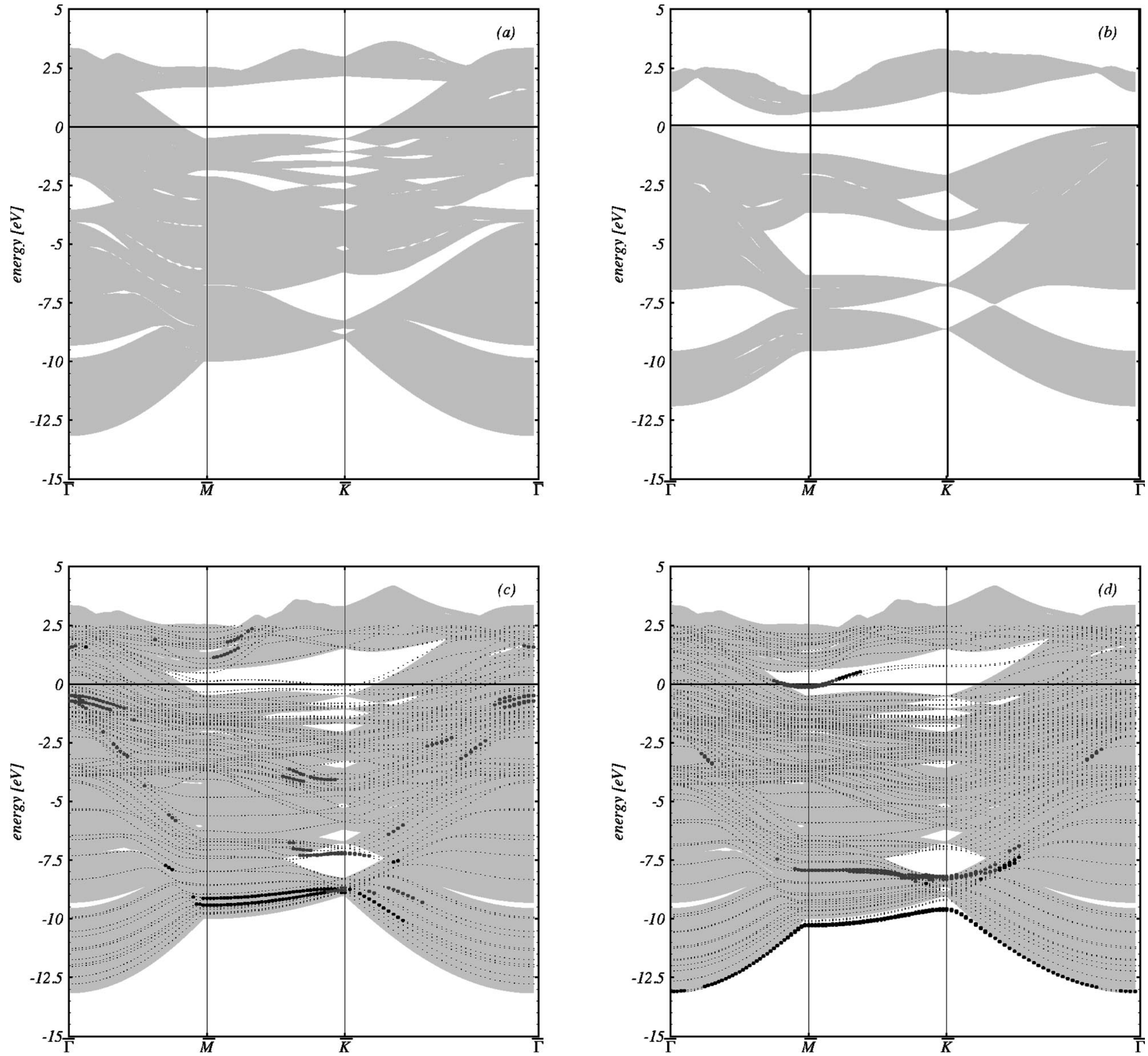

FIG. 2. Bulk bands projected along [111] orientation of bulk Si (a) and bulk $CoSi_2$ (b). Energy bands for the A7 (c) and A8 (d) interface types. Shaded area: sum of projected bands of (a) and (b). Interface states localized at positions $Si_C(I)$ (Si interface site of the $CoSi_2$ block): black circles; Si(I) (Si interface site of the Si block): grey circles. All other states: small dots. The fermi energy is defined by $E=0$ in all cases.

transmission through the interface, which requires conservation of energy and the Bloch vector component $\mathbf{k}_\parallel$ parallel to the interface orientation. Assuming an experimental Schottky barrier of ≈ 0.7 eV, it is argued that transmission for n-doped Si requires $CoSi_2$-like states at a conduction-band minimum of Si at ≈ 0.7 eV above E_F at $\mathbf{k}_\parallel \sim 0.85\times\overline{\bar{\Gamma}\text{-}\bar{M}}$. Also from our results, in agreement with Ref. 23, no projected states of bulk $CoSi_2$ exist in the interesting energy range [Fig. 2(b)].

By application of a kinematic theory (i.e. conservation of band energy and $\mathbf{k}_\parallel$) of ballistic electron emission microscopy (BEEM), Stiles and Hamann[24] utilized projected bands in the interface Brillouin zone to explain the delayed onset of transmission because they could obtain an appreciable overlap of $CoSi_2$ and Si states only about 0.9 eV above E_F (Fig. 2 of Ref. 24). Then it was even higher in energy by about 0.3–0.4 eV before states occured in $CoSi_2$ that corresponded to Si states at the conduction-band minimum with the same $\mathbf{k}_\parallel$. Inspecting our projected bands for the bulk cases, we obtain approximately the same result, because $CoSi_2$ bulk bands appear at ≈ 1.3 eV at the interesting $\mathbf{k}_\parallel$ [Fig. 2(b)]. So far, only bulk features were discussed. From our results for the interfaces in Figs. 2(c) and 2(d), we find a series of states in the interesting energy range at the discussed $\mathbf{k}_\parallel$. However, as far as we analyzed these states they are mainly of Si character, as will be discussed below for states at $\bar{M}$. This means, that even taking fully into account chemical bonding and relaxation, as we did by our supercell approach, does not alter the bulk-based picture of the delayed transmission. We want to point out, however, that we applied ground-state density-functional theory, which cannot ensure a quantitative meaning of unoccupied electronic states in particular.

Figures 2(c) and 2(d) show that the bands for the interface calculations also reveal interface-localized states. The definition of such states is somewhat ambigous because of the finite-slab (or repeated multilayer) construction we used. Since in our calculation the eigenstates are represented by plane waves, localized states must be defined by projections onto localized functions. This is done by expanding the plane waves into spherical functions inside spheres of radius 2.19 Å–corresponding to the assumed atomic radii—centered at the $\mathrm{Si}_C(I)$ position (black dots) and Si(I) positions (gray dots). For the sake of a useful graphical representation in Fig. 2, we defined interface states as states having at least 20% of their charge inside the chosen spheres. We discuss in detail only the bands for types A7 [Fig. 2(c)] and A8 (Fig. 2(d)], because the corresponding data for the B-type interfaces are rather similar.

Structure type A7 reveals very deep-lying interface localized states in the bulk projections, states in the lowest gap at $\bar{K}$, and gap states at and above Fermi energy for a wide range of $\mathbf{k}_{\|}$. Just above E_F at $\bar{M}$, two bands in the gap degenerate to a rather flat band along direction $\bar{M}$-$\bar{K}$, dispersing and splitting up when running from $\bar{K}$ to $\bar{\Gamma}$. No distinct localization—according to our definition given above—is observable. Also, the characteristic merging of bulk bands to a point at $\bar{M}$ is either shifted or blurred.

Quite in contrast to type A7, the bands of type A8 [Fig. 2(c)] change much less of the projected bulk band features. Just below E_F at $\bar{M}$ there is a distinct interface localized pair of bands. For A8 only one twofold-generated state arises in the gap, which visibly splits up between $\bar{M}$ and $\bar{K}$ due to coupling of the two interfacelike states becoming a nearly degenerate band without dispersion along direction $\bar{K}$-$\bar{\Gamma}$ before merging into the bulk projections. A remarkable feature is the deepest localized band along the boundary of the shaded bulk bands.

The band structure of both interface systems illustrates the pinning of E_F due to interface states in the gap. Whereas for type A7 [Fig. 2(c)] a very flat band of interface states along $\bar{M}$-$\bar{K}$ lies very close to Fermi energy, and is occupied at $\bar{K}$, for type A8 the pinning is due to dispersive interface bands at $\bar{M}$.

D. Interface states and metal-induced gap states

An important property of interface states is their z dependency orthogonal to the interface plane which is illustrated by planar averages of their spatial distribution. Averages over planes $\mathbf{r}_{\|}=\{x_{||},y_{||}\}$ parallel to the interface are defined by

$$\rho(z,E)=\frac{1}{A}\int_A \rho(\mathbf{r}_{\|},z,E)d\mathbf{r}_{\|}, \tag{6}$$

wherein A is the area of the corresponding two-dimensional unit cell and $\rho(\mathbf{r}_{\|},z,E)$ denotes the charge distribution of the electronic state at the chosen band energy E. The z axis obviously points in the [111] direction. Figures 3 and 4 show planar averages for selected states of interface types A7 and A8 at $\bar{M}$.

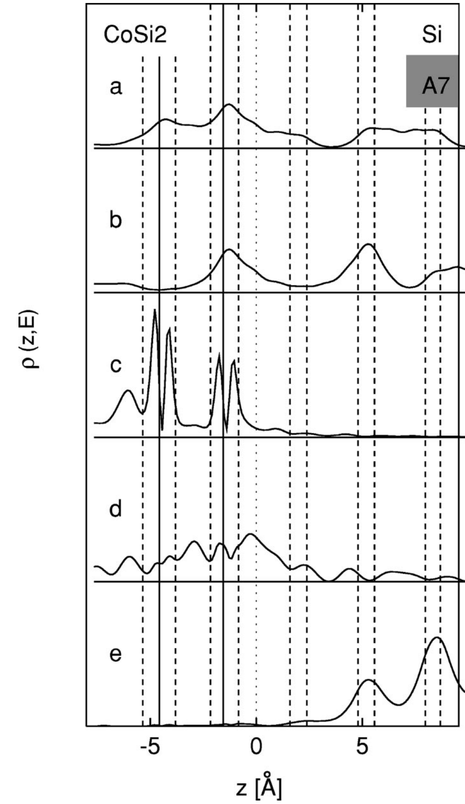

FIG. 3. Planar average of electron densities $\rho(z,E)$ of selected states at $\bar{M}$ for relaxed structure type A7 vs spacing z in direction [111]. Values of $\rho(z,E)$ are in arbitrary units. Values of z: distance with respect to the interface plane defined as half in between Si(I) and $\mathrm{Si}_C(I)$ according to Table II. The CoSi_2 block is at negative values of z, the Si block at positive z, and the interface plane at $z=0$ (dotted line). Si layers: dashed lines; Co layers: full lines. Selection of energies: (a) -9.42 eV, (b) -9.12 eV, (c) -0.34 eV, (d) 0.11 eV, and (e) 0.477 eV with respect to E_F.

In Fig. 3 the two lowest states at -9.42 (a) and -9.12 (b) eV fulfill the localization criterion. The density $\rho(z)$ in panel (a) is distributed into two distinctly separated regions. In the CoSi_2 block two distinct maxima at Co layers occur, but some appreciable density is still found in the interface region. The minimum in the Si block separates the pair of planes closest to the interface from the bulklike planes. At the $\mathrm{Si}_C(I\text{-}1)$ location with $z=-1.24$ Å, $\rho(z)$ is large, giving the state its localization character. Panel (b) reveals a state of strongly localized peaks at $\mathrm{Si}_C(I)$ and Co(I-1) plane positions, and values of z corresponding to the first two Si bulk layers with very small intensity at Si(I) and Si(I-1) close to the interface. Summarizing, both states discussed are of CoSi_2 as well as Si character.

The properties of the remaining three states are distinctly different: The states in panels (c) and (d) are of CoSi_2 character, whereas state (e) is well localized within the Si block. State (c) at -0.34 eV is just in the center of the energy gap and characteristic for a metal-induced gap state (MIGS). A pair of sharp peaks arises twice: at the positions of $\mathrm{Si}_C(I)$ and Co(I-1), and the corresponding sites in the next CoSi_2 trilayer. A small but distinct nonzero $\rho(z)$ decays into the Si block up to 5 Å away from the interface. Closer inspection of the bands in Fig. 2(c) shows that this state is by far not

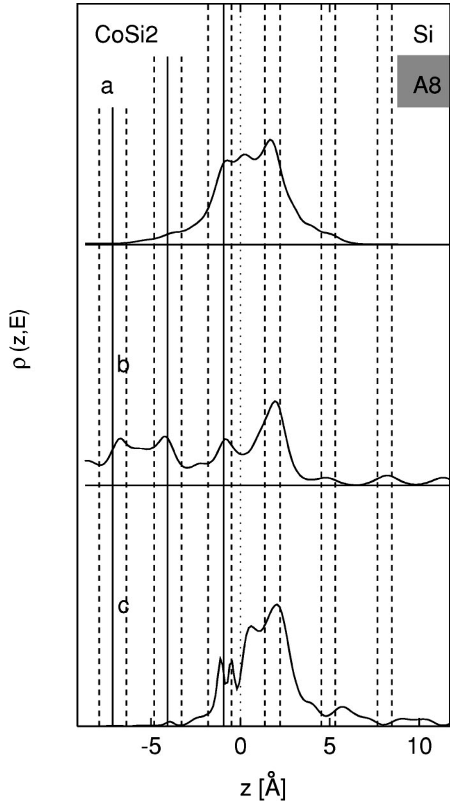

FIG. 4. Planar averages of electron densities of selected states for relaxed structure type A8 at $\bar{M}$. For details, see Fig. 3. Selection of energies: (a) -10.30 eV, (b) -7.94 eV, and (c) -0.14 eV with respect to E_F.

doubly degenerate, which must be the case if it would be a truly localized interface state: about 0.3 eV deeper a state is found belonging to an energy band which finally merges at $\bar{K}$ with the band to which state (c) belongs. The deeper state lies already in the bulk continuum, and we cannot distinguish sharply between states resonant in a bulk block and a new state being generated by the interface.

State (d) at 0.11 eV just above the Fermi energy is of rather diffuse character with some small but long-ranged tails in the Si block. This state at $\bar{M}$ in the center of the gap is a well-defined localized interface state because two bands are nearly perfectly degenerate. Due to its charge distribution, it is of MIGS character.

Finally, state (e) at 0.48 eV is of Si character without being a truly localized interface state because—again—it is by far not degenerate. Even its intensity at the interface planes is smaller than at the bulklike layers.

Discussing the results presented in Fig. 4 for structure type A8, we derive quite a different charge distribution character of interface states. The state (a) of lowest energy at -10.30 eV shows perfect localization in the interface layers of both blocks. Accordingly, the band structure reveals two nearly degenerate bands spanning all the shown $\mathbf{k}_\parallel$ directions. Although $\rho(z)$ is larger at Si(I) than at $Si_C(I)$, in the band structure it is denoted to be of Si_C character due to the definition of localization for the band structure for which we integrated over atomic spheres.

At -7.94 eV in panel (b) of Fig. 4, a state of $CoSi_2$ character is found which induces quite some charge at the first two interface layers of Si. In the band structure it is denoted as a state fulfilling the localization criterion in the Si(I) sphere. It seems surprising that this state decays rather fast toward the Si block, because inspecting the projected bulk bands of Si at $\bar{M}$ no energy gap is found between -7.5 and -8 eV [Fig. 2(a)]. Closer inspection, however, shows that it might be possible that due to the curvature of the shaded energy regions just at this critical energy a very small forbidden energy range arises.

The distinct interface state in Fig. 2(d) at -0.14 eV is strikingly manifested by $\rho(z)$ in panel (c) of Fig. 4: it is strongly localized at layers $Si_C(I)$ and Co(I) and Si(I) and Si(I-1). At the $CoSi_2$ interface just at the interface layer positions we find the characteristic two-peak structure.

By summation of all states of the interface systems in the energy window defined by the valence-band maximum and conduction-band minimum of Si, we derive the charge density ρ_{MIGS} comprising all the metal-induced gap states. From the planar and macroscopically[25] averaged ρ_{MIGS}, we derive decay lengths λ which describe the decay of metallic $CoSi_2$ states into the Si block. The values of λ are 3.2 and 3.0 Å for types A7 and B7, correspondingly, being rather similar and substantially shorter than $\lambda=4.8$ and 3.9 Å for types A8 and B8. The longer-ranged character of ρ_{MIGS} of the eightfold-coordinated interface types is due to localized interface states as shown, for example, in Fig. 4(c).

E. Schottky barriers

In our study, Schottky barrier heights are derived from two different approaches: the first is based on the lineup of averages of electrostatic potentials,[25] and the second utilizes the shift of localized Si bulk states due to the presence of the interface.

In general, the Schottky barrier height Φ_p for p-doped semiconductors is defined by the difference between the Fermi energy of the metal E_F^M and the valence-band maximum of the semiconductor E_V^S:

$$\Phi_p = E_F^M - E_V^S. \tag{7}$$

The barrier height Φ_n for n-doped semiconductors is then correspondingly defined by

$$\Phi_n = E_{gap} - \Phi_p, \tag{8}$$

when E_{gap} is the measured energy gap of the semiconductor. The barrier height Φ_p might be reformulated as[25,26]

$$\Phi_p^{av} = \Delta E^{bulk} + \Delta V. \tag{9}$$

The difference ΔE_{bulk} is then expressed by

$$\Delta E^{bulk} = (E_F^{M,bulk} - V_{av}^{M,bulk}) - (E_F^{S,bulk} - V_{av}^{S,bulk}) \tag{10}$$

where the first term denotes the energy difference between the Fermi level of the metal and its average electrostatic potential, and the second term is the corresponding difference for the semiconductor. Both terms in Eq. (10) are derived separately for the corresponding bulk systems. In our case we obtain a value $\Delta E^{bulk} = 3.26$ eV.

The potential lineup ΔV is the shift due to interface formation of the averaged electrostatic potentials $V_{av}^{M,int}$ and

$V_{av}^{S,int}$ for the metal and semiconductor phases, accordingly. Naturally, it has to be derived from the actual interface calculations:

$$\Delta V = V_{av}^{M,int} - V_{av}^{S,int}. \tag{11}$$

The quantity Φ_p^{av} can be derived from pseudopotential calculations in a straightforward manner. However, the calculation of ΔV needs some care in order to get rid of the artificial choice of the interface plane. The interface plane is introduced just as a simple geometrical concept, but has no meaning for the electronic states which are smooth over the whole space. To evaluate ΔV now from electrostatic potentials given in real space, the procedure for macroscopic averaging according to Ref. 25 is strictly defined. By that, the macroscopic average $\bar{f}(z)$ of a function $f(z)$, which denotes a planar average similar to Eq. (6), is obtained by the convolution

$$\bar{f}(z) = \frac{1}{a}\int_{z-a/2}^{z+a/2} f(z')dz', \tag{12}$$

in which a denotes the period in z direction of the considered system. A further complication arises when the actual interface system consists of two bulk blocks with nonmatching lattices, i.e., different periods in the z direction. Then, a twofold convolution has to be applied,[25] resulting in a macroscopic averaged function $\bar{\bar{f}}(z)$. In general, for a bulk with perfect bulk periodicity in the z direction, the macroscopic average is a constant independent of z. We checked that for the separated bulk systems of $CoSi_2$ and Si stacked according to the [111] orientation.

In the present case, there are two different periods of z, namely, 9.22 Å for $CoSi_2$ and 9.36 Å for Si. We studied two different averaging procedures, as shown in Fig. 5. Procedure (1), which is a single average changing the period a abruptly when moving from the $CoSi_2$ block to Si; and procedure (2) which performs the rigorous twofold convolution. In general for the averaging we used the sum of electronic and ionic potentials because—as pointed out by Baroni *et al.*[25]—Poisson's equation has to be solved for the total charge, electronic as well as ionic charge, in order to derive a physically meaningful electrostatic potential. Figure 5 shows the results for A7 and A8 interface types only, because for B-type interfaces very similar results are obtained, correspondingly.

Procedure (1) yields smooth averages in the center of the Si block, very small kinks at the (artificial) interface plane and fluctuations inside the $CoSi_2$ block at Co layer positions. Procedure (2) results in very smooth and broad curves. What is needed for the determination of ΔV is the value of the averaged potential deep in the bulk far away from the interface, i.e., at the centers of the respective blocks. Analyzing the Si block in Fig. 5, we can extract well-defined values from procedures (1) and (2) yielding the same values within a difference of 0.04 eV. The results for the $CoSi_2$ block are, however, less clear. The twofold average is moved to less negative values compared to procedure (2) presumably because the $CoSi_2$ block is too thin: the broad width of the convolution function might smear out too much of the negative valley. Procedure (2) results in a fluctuating ΔV, making a choice for the lineup somewhat arbitary within 0.2 eV. For

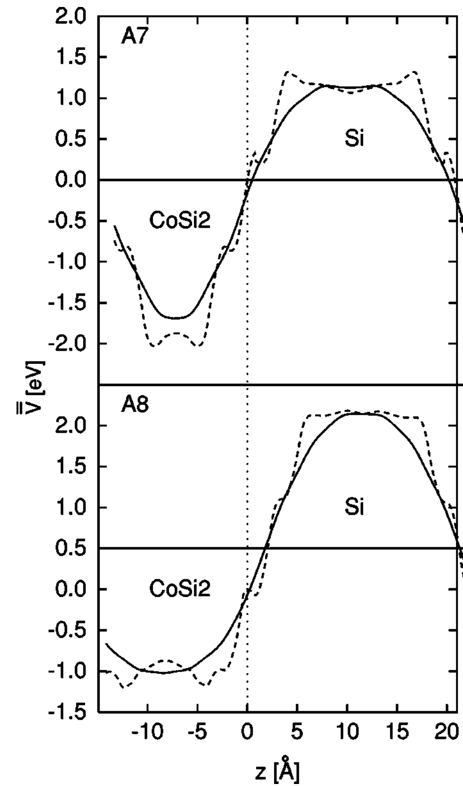

FIG. 5. Macroscopic average of the electrostatic potential according to procedures (1) (dashed line) and (2) (solid line) (see text) for interface types A7 and A8 vs spacing z in direction [111]. The potential is shifted by a constant so that $\int \Delta V\, dz = 0$. Positive values of z: Si block; negative values: $CoSi_2$ block.

type A8, the twofold average seems to work reasonably, being no more negative at the $CoSi_2$ center than the again fluctuating result for procedure (2). Because in the $CoSi_2$ block curve (2) is higher (lower) than curve (1), the corresponding lineup ΔV is less (more) negative for type A7 (A8), and the barrier heights change correspondingly in Table IV. In Ref. 25 the averaging method was introduced for GaAs(100)/AlAs(100) interfaces, where the perturbation caused by the interface is much faster screened out than for $CoSi_2(111)/Si(111)$ interfaces as discussed.

In all-electron *ab initio* calculations another procedure might be adopted for calculating Schottky barrier heights. There one derives the energies of core states, and compares their values for the pure bulk systems (with respect to Fermi energy for the metal and valence-band maximum for the semiconductor) to the corresponding values of the interface system.[30] Because of the strong localization of proper core states (typically, $1s$ states are chosen) the relative changes of core levels is—in first order—due to the change of the average electrostatic potential in the atomic spheres. This change reflects the potential lineup due to the interface, if the potential is averaged in atomic spheres around bulklike atomic positions (in the center of the blocks).

In our case of a pseudopotential approach, it is not obvious how to find localized states because core states are frozen and only used for the construction of the pseudopotential. However, as discussed in Sec. III C for the projected energy bands of pure bulk Si at $\bar{K}$, some localization in **k** space occurs. Now analyzing the interface band structures,

TABLE IV. Potential lineups ΔV and p-type Schottky barrier heights Φ_p in eV. ΔV^1 and Φ_p^{av1} are derived from averaging procedure (1). ΔV^2 and Φ_p^{av2} are derived from averaging procedure (2). Φ_p^{loc} is derived from bulk, localized Si 3s-states. $\Phi_p^{QP,i}$ is the sum of Φ_p^i and quasiparticle corrections of 0.31 eV. For further details, see text. The experimental value of Φ_p is 0.66 eV.

	A7	B7	A8	B8
ΔV^1	-2.91	-3.09	-3.06	-3.29
ΔV^2	-2.82	-2.98	-3.16	-3.49
Φ_p^{av1}	0.35	0.17	0.20	-0.03
Φ_p^{av2}	0.44	0.28	0.10	-0.18
Φ_p^{loc}	0.24	0.05	0.13	-0.06
$\Phi_p^{QP,av1}$	0.66	0.48	0.51	0.28
$\Phi_p^{QP,av2}$	0.75	0.59	0.41	0.13
$\Phi_p^{QP,loc}$	0.55	0.36	0.44	0.25

we again detect similar band mergings of selected bands at about -8.5 eV. All these states are of Si 3s character. Analyzing the averaged density $\rho(z)$ for these 3s states for all four interface types, we find that $\rho^{Si\text{-}3s}(z)$ is perfectly localized in the Si block. Therefore, if Si bulklike states in the interface systems experience some change of $\bar{V}$ (now averaged not in an atomic sphere but in a Si bulklike block), this change is directly reflected in the corresponding Kohn-Sham energies.

The discussed localization property can now be exploited to define the Schottky barrier height by

$$\Phi_p^{loc} = \epsilon_{bulk}^{Si-3s} - \epsilon_{int}^{Si-3s}, \qquad (13)$$

where ϵ_{bulk}^{Si-3s} is the Kohn-Sham eigenvalue of the Si 3s state with respect to E_F (which is equal to E_V) of the pure Si bulk. In Fig. 2(b) this is the lowest energy where all bands merge at $\bar{K}$. The energy ϵ_{int}^{Si-3s} is the Kohn-Sham level of the same state with respect to E_F of the interface system. Values for Φ_p^{loc} are given as the last row in Table IV. These values compare reasonably well with the results obtained using the macroscopic averages of the electrostatic potential. The qualitative trends are the same, where the largest barrier is predicted for type A7, a slightly negative value is predicted for type B8, and Φ_p for type A8 is larger than that for B7. As in Sec. III D, not taking into account a quasiparticle correction, all our calculated barrier heights are substantially lower than the experimentally accepted result.

All values calculated by the procedures discussed above are significantly smaller than the accepted experimental value of 0.66 eV (derived from BEEM data[27]), because the Kohn-Sham or density-functional-theory (DFT) barrier heights (as we calculated) have to be corrected due to the relative band bending of DFT bands to the quasiparticle bands.[28] The DFT barrier is too small by an amount Γ_p for p type barriers and Γ_n for n-type barriers. The sum $\Gamma_p + \Gamma_n = \Delta$ equals the difference $\Delta = E_{gap} - E_{gap}^{DFT}$, the difference between the experimental (or quasiparticle) value and the value E_{gap}^{DFT} derived from standard DFT calculations for the ground state. In principle, such quasiparticle corrections for the separate bulk systems need to be calculated. For $CoSi_2$ such calculations still need to be done. Following arguments in the comment by Godby *et al.*[29] for $NiSi_2$/Si interfaces, we assume that the quasiparticle correction for $CoSi_2$ is vanishing, and that $\Gamma := \Gamma_p = \Gamma_n$. Then the correction $\Gamma = \Delta/2$ in our case amounts to 0.31 eV. Adding this constant to our calculated values we come substantially closer to the experimental value, in particular for the A7 type and also for B7 and A8 types, as listed in Table IV. It should be noted that, due to the rather crude estimation of the quasiparticle correction, the absolute values of the calculated barriers contain some uncertainties, presumably on the order of 0.1–0.2 eV. The calculated trend of barrrier height versus geometry, however, seems to be meaningful.

As listed in Table IV, the barrier heights for the sevenfold-coordinated interface types are always larger than the results for their corresponding eightfold counterparts. Also, Φ_p for the A-type interfaces is significantly larger by about 0.2 eV than for B-type interfaces. We conclude that the Schottky barrier height depends on the geometry of the interface. Recently it was stated also by means of *ab initio* calculations that the Schottky barrier height depends on the nature of the metal,[31] the crystallographic orientation, and the microscopic morphology of the interface,[32] rather than depending on the nature of the semiconductor only. Concerning the theoretical calculation of Schottky barrier heights for silicide/Si interfaces, Fujitani and Asano[33] claimed that their value depends crucially on the cell size in a repeated slab scheme. On the other side, Das *et al.*[34] argued that the assumed layer thicknesses for their calculations on $NiSi_2(111)/Si(111)$ is sufficient. Magaud-Martinage *et al.*[35] calculated barrier heights for $CoSi_2(111)/Si(111)$ and $NiSi_2(111)/Si(111)$ in reasonable agreement with experiment using a self-consistent tight-binding method coupled with a decimation technique which does not require translational periodicity in the direction perpendicular to the interface.

IV. SUMMARY

Based on a powerful *ab initio* method, we tried to model the $CoSi_2(111)/Si(111)$ interface by studying four possible structure types. For the experimentalist it would be very helpful to know which structure type is the most stable one. For that reason we investigated interface energies rather extensively, with the result that after relaxing the atomic posi-

tions all four types are energetically very close, the eightfold types being slightly more favored by 0.05–0.10 eV. Therefore, we conclude that kinetics plays an important role during the actual growth of a particular type of interface. The situation is even more complicated when we look at the calculated Schottky barrier heights. Then, it seems that type A7 is closest to experiment, the other values—in particular for type B8—being significantly smaller. However, one should keep in mind that our estimate for the quasiparticle correction is rather crude. Furthermore, when deriving the potential lineup according to Eq. (11) in particular for A7 and B7 interfaces, we find by performing the macroscopic averaging according to Ref. 25—as one should do in order to be independent from artificial choices of the interface plane—that the thickness of the $CoSi_2$ block is possibly too small, leaving some additional uncertainty as to the final value for the barrier height. The electronic structure, in particular for the eightfold types, comprises states strongly localized at the interface. The decay length of metal-induced gap states is significantly different, about 3 Å for the sevenfold interface types, but substantially longer ranged for types A8 (about 5 Å) and B8 (about 4 Å).

ACKNOWLEDGMENTS

Work was supported by the Austrian Science Foundation (FWF) under Project No. P10645-PHY. We also thank the Center for Computational Materials Science (CMS) for support. Thanks also to W. Weiss, K. Reuter, E.G. Moroni, and W. Wolf for very helpful discussions. Partial support was given by the Austrian Ministry of Science under Project No. GZ 49.975.

[1] R. Tung, Mater. Chem. Phys. **32**, 107 (1992).
[2] H. Sirringhaus, E. Y. Lee, and H. von Känel, J. Vac. Sci. Technol. B **12**, 2629 (1994); P. Werner, W. Jäger, and A. Schüppen, J. Appl. Phys. **74**, 3846 (1993), and references therein.
[3] S. Mantel, Mater. Sci. Rep. **8**, 1 (1992).
[4] R. Stadler, W. Wolf, R. Podloucky, G. Kresse, and J. Hafner, Phys. Rev. B **54**, 1729 (1996).
[5] D. Vogtenhuber and R. Podloucky, Phys. Rev. B **55**, 10 805 (1997).
[6] R. Stadler, R. Podloucky, G. Kresse, and J. Hafner, Phys. Rev. B **57**, 4088 (1998).
[7] H. v. Känel, Mater. Sci. Rep. **8**, 193 (1992).
[8] J. M. Gibson, J. C. Bean, J. M. Poate, and R. T. Tung, Appl. Phys. Lett. **41**, 818 (1982).
[9] A. Catana, P. E. Schmid, S. Rieubland, F. Levy, and P. Stadelmann, J. Phys.: Condens. Matter **1**, 3999 (1989).
[10] C. W. T. Bulle-Lieuwma, A. F. de Jong, A. H. vsn Ommen, J. F. van der Veen, and J. Vrijmoeth, Appl. Phys. Lett. **55**, 648 (1989).
[11] D. R. Hamann, Phys. Rev. Lett. **60**, 313 (1988).
[12] G. Kresse and J. Hafner, Phys. Rev. B **48**, 13 115 (1993); **49**, 14 251 (1994); **54**, 11 169 (1996); G. Kresse and J. Furthmüller, Comput. Mater. Sci. **6**, 15 (1996).
[13] D. Vanderbilt, Phys. Rev. B **41**, 7892 (1990).
[14] G. Kresse and J. Hafner, J. Phys.: Condens. Matter **6**, 8245 (1994).
[15] E. G. Moroni, G. Kresse, J. Hafner, and J. Furthmüller, Phys. Rev. B **56**, 15 629 (1997).
[16] S. G. Louie, S. Froyen, and M. L. Cohen, Phys. Rev. B **26**, 1738 (1982).
[17] H. J. Monkhorst and J. d. Pack, Phys. Rev. B **13**, 5188 (1976).
[18] M. Methfessel and A. T. Paxton, Phys. Rev. B **40**, 3616 (1989).
[19] A. D. Becke, Phys. Rev. A **38**, 3098 (1988); J. P. Perdew, Phys. Rev. B **33**, 8822 (1986).
[20] P. J. van den Hoek, W. Ravenek, and E. J. Baerends, Phys. Rev. Lett. **60**, 1743 (1988); Surf. Sci. **205**, 549 (1988).
[21] W. Weiss, Ph.D. thesis, University of Erlangen-Nürnberg, 1998.
[22] K. Heinz, M. Kottcke, U. Löffler, and R. Döll, Surf. Sci. **357-358**, 1 (1996); P. J. Rous, J. B. Pendry, D. K. Saldin, K. Heinz, K. Müller, and N. Bickel, Phys. Rev. Lett. **57**, 2951 (1986); P. J. Rous, Prog. Surf. Sci. **39**, 3 (1992).
[23] L. F. Mattheis and D. R. Hamann, Phys. Rev. B **37**, 10 623 (1988).
[24] M. D. Stiles and D. R. Hamann, J. Vac. Sci. Technol. B **9**, 2394 (1991).
[25] A. Baldereschi, S. Baroni, and R. Resta, Phys. Rev. Lett. **61**, 734 (1988); S. Baroni, R. Resta, A. Baldereschi, and M. Peressi, in *Spectroscopy of Semiconductor Microstructures*, Vol. 206 of *NATO Advanced Study Institute, Series B: Physics*, edited by G. Fasol, A. Fasolino, and P. Luigi (Plenum, New York, 1989), p. 251.
[26] R. G. Dandrea and C. B. Duke, J. Vac. Sci. Technol. A **11**, 848 (1993); J. Vac. Sci. Technol. B **11**, 1553 (1993).
[27] H. Sirringhaus, E. Y. Lee, and H. v. Känel, Phys. Rev. Lett. **73**, 577 (1994); T. Meyer and H. v. Känel, *ibid.* **78**, 3133 (1997).
[28] R. W. Godby and L. J. Sham, Phys. Rev. B **49**, 1849 (1994).
[29] R. W. Godby, L. J. Sham, and M. Schlüter, Phys. Rev. Lett. **65**, 2083 (1990).
[30] S. Picozzi, A. Continenza, S. Massidda, and A. J. Freeman, Phys. Rev. B **57**, 4849 (1998).
[31] M. van Schilfgaarde, E. R. Weber, and N. Neumann, Phys. Rev. Lett. **65**, 2728 (1990); J. Vac. Sci. Technol. B **9**, 2140 (1991).
[32] R. J. Needs, J. P. A. Charlesworth, and R. W. Godby, Europhys. Lett. **25**, 81 (1994).
[33] H. Fujitani and S. Asono, J. Phys. Soc. Jpn. **57**, 2253 (1988); Appl. Surf. Sci. **41/42**, 164 (1989); Phys. Rev. B **42**, 1696 (1990).
[34] G. P. Das, P. Blöchl, O. K. Andersen, N. E. Christensen, and O. Gunnarsson, Phys. Rev. Lett. **63**, 1168 (1989).
[35] L. Magaud-Martinage, D. Mayou, A. Pasturel, and F. Cyrot-Lackmann, Surf. Sci. **256**, 379 (1991).